APPLICATIONS OF EXTENDED HIGHER ORDER SANDWICH PANEL THEORY
FOR PLATES WITH ARBITRARY ASPECT RATIOS

Faisal Siddiqui and George A. Kardomateas

msp

APPLICATIONS OF EXTENDED HIGHER ORDER SANDWICH PANEL THEORY FOR PLATES WITH ARBITRARY ASPECT RATIOS

FAISAL SIDDIQUI AND GEORGE A. KARDOMATEAS

In this paper, solutions for a transversely loaded simply supported case with several different plate configurations based on extended higher-order sandwich panel theory (EHSAPT) are outlined and numerical results are presented. The results are also compared to established elasticity solutions and validation of EHSAPT for plates of arbitrary aspect ratios is made. The results are also compared to existing classical and first-order shear models for completeness. The results show excellent agreement both for displacements and stresses through the core. Analytical formulations and solutions to the natural frequency analysis of simply supported composite sandwich plates are also presented. The effects of variation of geometrical parameters of the structure on the natural frequency are also studied.

1. Introduction

This paper deals with the application of extended higher-order sandwich panel theory for plates with arbitrary aspect ratios derived in the companion paper [SK 2019]. The face sheets are made up of two individual laminas, each of which can have different layouts. The results have been presented for a transversely loaded simply supported sandwich panel, for static and dynamic cases, and are then compared to the classical model, the first order shear model [Plantema 1966; Allen 1969] and elasticity solutions [Kardomateas and Phan 2011; Kardomateas 2008; Noor 1973]. After establishing accuracy of the theory we then study the effects of varying certain geometric parameters on the fundamental natural frequency of the structure.

SK [2019] proposed an extended higher-order sandwich panel theory for sandwich plates with arbitrary aspect ratios considering a transverse displacement in the core that varies as a second-order equation in z and the in-plane displacements that are of third order in z, the transverse coordinate.

A higher-order sandwich panel theory (HSAPT) for one-dimensional beam was proposed in [Frostig et al. 1992], which considers the shear strain in the core to be constant while the resulting normal strain in the core is linear in z. Another model presented by Hohe et al. [2006] for sandwich plate considers the resulting transverse normal strain as constant in the transverse coordinate, z, while the shear strains are first order in z. Another higher-order theory proposed by Li and Kardomateas [2008] considers the transverse normal strain as third order in z, and the shear strains as fourth order in the transverse coordinate. Phan et al. [2012] extended the HSAPT theory [Frostig et al. 1992] for beams that allows for the transverse shear distribution in the core to acquire the proper distribution as the core stiffness increases as a result of nonnegligible in-plane stresses. The HSAPT model is incapable of capturing the in-plane stresses and assumes negligible in-plane rigidity. The current research extends that concept and applies it to two-dimensional plate structures with variable aspect ratios. This approach allows for five

---

generalized coordinates in the core. Noor [1973] presented an exact three dimensional elasticity solution for the free vibration analysis of isotropic, orthotropic and anisotropic composite laminated plates which serves as a benchmark for comparison with these extended higher order theories.

2. Application of EHSAPT to a simply supported sandwich plate: static case

We consider a sandwich plate with two identical face sheets of thickness f and a core of thickness $2c$ respectively. The cartesian coordinate system is placed in the middle plane of the sandwich plate as shown in Figure 1. The corresponding displacements are denoted (u, v, w). The subscripts t, b and c refer to the top face sheet, bottom face sheet and the core respectively. Similarly, the subscript 0 refers to the middle surface of the respective phase. The total thickness of the plate is given by $h_{\text{tot}} = 2f + 2c$.

In order to compare the results of EHSAPT with other available theories, the case of a simply supported plate will be studied. The following boundary conditions are applied [SK 2019]: For $x = 0, a$,

$$u_0^t = u_0^c = u_0^b = 0, \quad v_0^t = v_0^c = v_0^b = 0, \quad w^t = w_0^c = w^b = 0, \quad \tilde{M}^t = \tilde{M}^c = \tilde{M}^b = 0. \quad (2\text{-}1)$$

Similar boundary conditions can be written for the other two ends of the plate at $y = 0, b$.

The displacements can be written in the form

$$u_0^t = U^T \cos \frac{m\pi x}{a} \sin \frac{n\pi y}{b}, \qquad u_0^c = U^C \cos \frac{m\pi x}{a} \sin \frac{n\pi y}{b}, \qquad u_0^b = U^B \cos \frac{m\pi x}{a} \sin \frac{n\pi y}{b}, \qquad (2\text{-}2\text{a})$$

$$v_0^t = V^T \sin \frac{m\pi x}{a} \cos \frac{n\pi y}{b}, \qquad v_0^c = V^C \sin \frac{m\pi x}{a} \cos \frac{n\pi y}{b}, \qquad v_0^b = V^B \sin \frac{m\pi x}{a} \cos \frac{n\pi y}{b}, \qquad (2\text{-}2\text{b})$$

$$w^t = W^T \sin \frac{m\pi x}{a} \sin \frac{n\pi y}{b}, \qquad w_0^c = W^C \sin \frac{m\pi x}{a} \sin \frac{n\pi y}{b}, \qquad w^b = W^B \sin \frac{m\pi x}{a} \sin \frac{n\pi y}{b}, \qquad (2\text{-}2\text{c})$$

$$\phi = \Phi \sin \frac{m\pi x}{a} \cos \frac{n\pi y}{b}, \qquad \psi = \Psi \cos \frac{m\pi x}{a} \sin \frac{n\pi y}{b}. \qquad (2\text{-}2\text{d})$$

Here U^T, U^C, U^B, V^T, V^C, V^B, W^T, W^C, W^B, Φ and Ψ are constants to be determined. Substituting equations (2-2) into the governing differential equations [SK 2019] results in a system of eleven equations for the eleven unknown constants: U^T, U^C, U^B, V^T, V^C, V^B, W^T, W^C, W^B, Φ and Ψ.

2A. *Numerical results and case study.* In this section, we present the numerical results for several typical sandwich configurations. The results are compared to the classical model, the first-order shear model and established elasticity solutions. In the following we assume a sinusoidal transverse loading
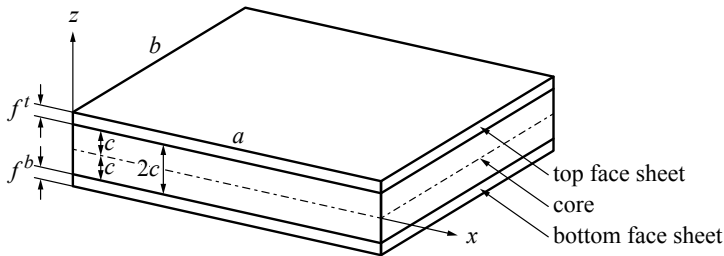

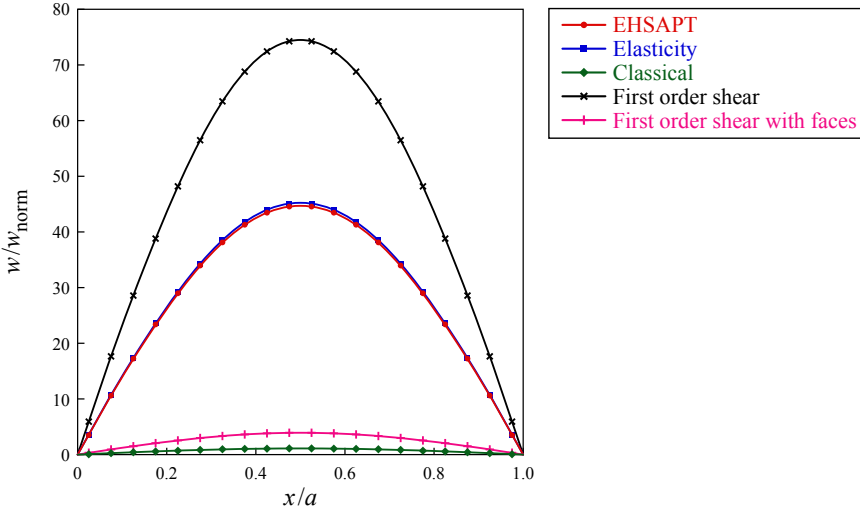**Figure 1.** Geometric configuration of the plate.

Figure 2. Transverse displacement w^t at the top face $z = c + f^t$ at $y = \frac{1}{2}b$ for $a = b = 5h_{\text{tot}}$.

on the top face sheet of the form

$$q(x, y) = q_0 \sin \frac{\pi x}{a} \sin \frac{\pi y}{b}, \quad 0 \leq x \leq a, \quad 0 \leq y \leq b, \tag{2-3}$$

where q_0 is the magnitude of the load applied which is taken to be 10^6. Let us consider a sandwich configuration consisting of unidirectional graphite/epoxy faces with moduli (in GPa) of $E_1^f = 181.0$, $E_2^f = E_3^f = 10.3$, $G_{12}^f = G_{31}^f = 7.17$ and $G_{23}^f = 5.96$ and Poisson's ratio of $v_{12}^f = 0.277$, $v_{31}^f = 0.016$ and $v_{32}^f = 0.4$. The core is made up of hexagonal glass/phenolic honeycomb with moduli (in GPa) of $E_1^c = E_2^c = 0.032$, $E_3^c = 0.300$, $G_{23}^c = G_{31}^c = 0.048$, and $G_{12}^c = 0.013$ and Poisson's ratio of $v_{12}^c = v_{31}^c = v_{32}^c = 0.250$.

The two face sheets are assumed to be identical with a thickness of $f_t = f_b = f = 2\,\text{mm}$. The core thickness is $2c = 16\,\text{mm}$. The total thickness of the plate is defined to be $h_{\text{tot}} = 2f + 2c$. In the following results, the displacements are normalized with $100 \times h_{\text{tot}} q_0 / E_1^f$ and the normal stresses with $q_0 a^2 / h_{\text{tot}}^2$.

Two plate configurations are considered with $a = b = 5h_{\text{tot}}$ and $a = b = 20h_{\text{tot}}$ respectively. Plotted in Figure 2 is the normalized displacement at the top face sheet as a function of x at $y = \frac{1}{2}b$. In this figure we also show the predictions of the classical plate theory as well as the first-order shear theories; for the latter, there are two versions: one that is based only on the core shear stiffness and one that includes the face sheet stiffnesses. From Figure 2, we can see that both the classical and the first-order shear theories seem to be inadequate. The classical theory is too nonconservative and can sometimes hardly make any difference. On the other hand, the first-order shear theory where shear is assumed to be carried exclusively by the core is too conservative; this clearly demonstrates the need for higher-order theories in dealing with sandwich plate structures. In this regard the EHSAPT theory gives a profile which is essentially identical to the elasticity solution. In Figure 2 we can also see the effect of transverse shear, which is an important feature of sandwich structures.
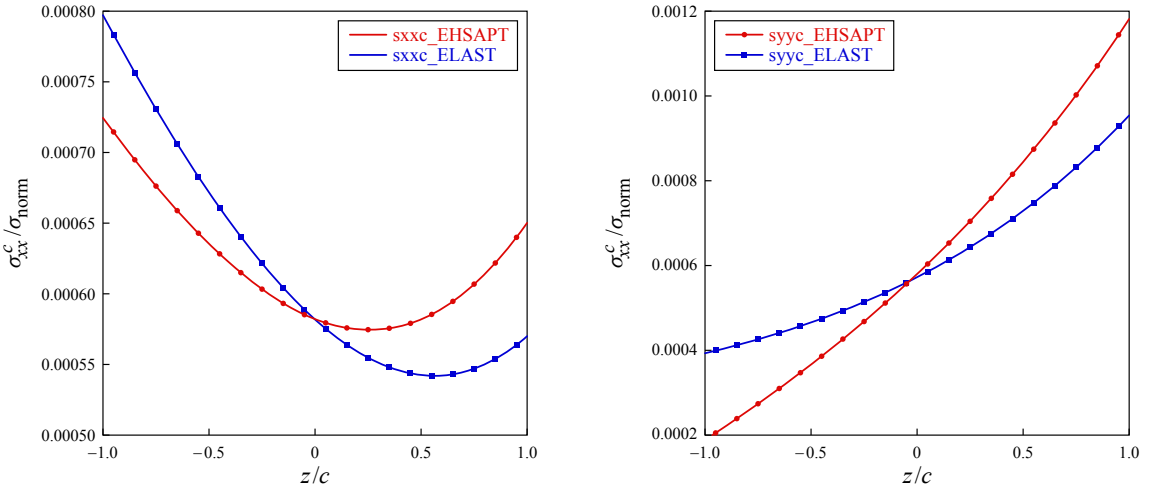
Figure 3. Through-thickness distribution in the core of the axial stress: σ_{xx} (left) and σ_{yy} (right) at $x = \frac{1}{2}a$ and $y = \frac{1}{2}b$; case of $a = b = 5h_{\text{tot}}$.
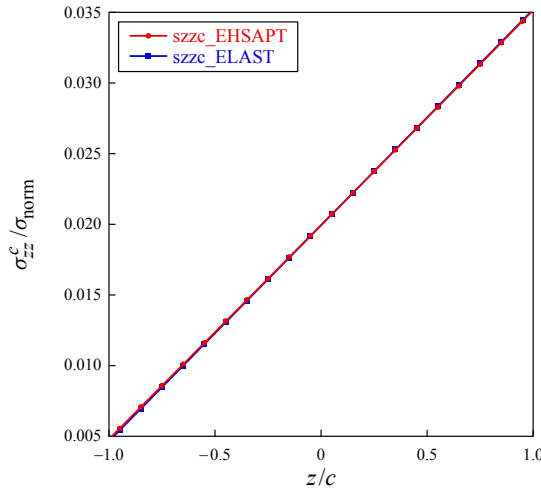

Figure 4. Through-thickness distribution in the core of the transverse normal stress σ_{zz} at $x = \frac{1}{2}a$ and $y = \frac{1}{2}b$; case of $a = b = 5h_{\text{tot}}$.

The distribution of the axial stresses σ_{xx} and σ_{yy} in the core as a function of z at the midspan location, $x = \frac{1}{2}a$ and $y = \frac{1}{2}b$ (where the bending moment is maximum) is plotted in Figure 3. Note that for both elasticity and the extended high-order theory, there is no symmetry with regard to the midplane ($z = 0$).

The through-thickness distribution of the transverse normal stress in the core, σ_{zz}, at the midspan location, $x = \frac{1}{2}a$ and $y = \frac{1}{2}b$, is shown in Figure 4. It can be seen that the elasticity curve is in perfect agreement with the EHSAPT curve and both are nearly linear.

Plotted in Figures 5, 6 and 7 are the normalized displacement, axial stresses and the transverse normal stress respectively for the case of $a = b = 20h_{\text{tot}}$.
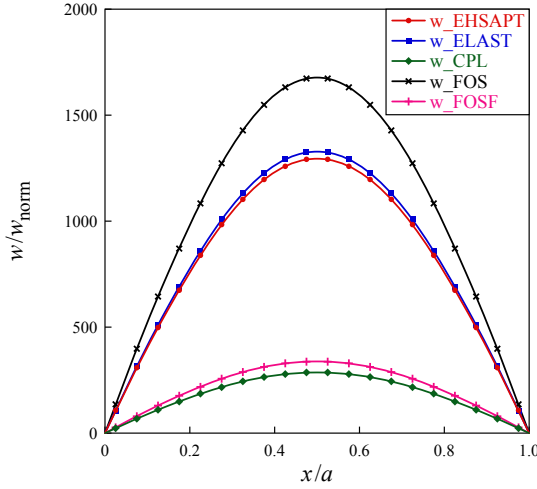
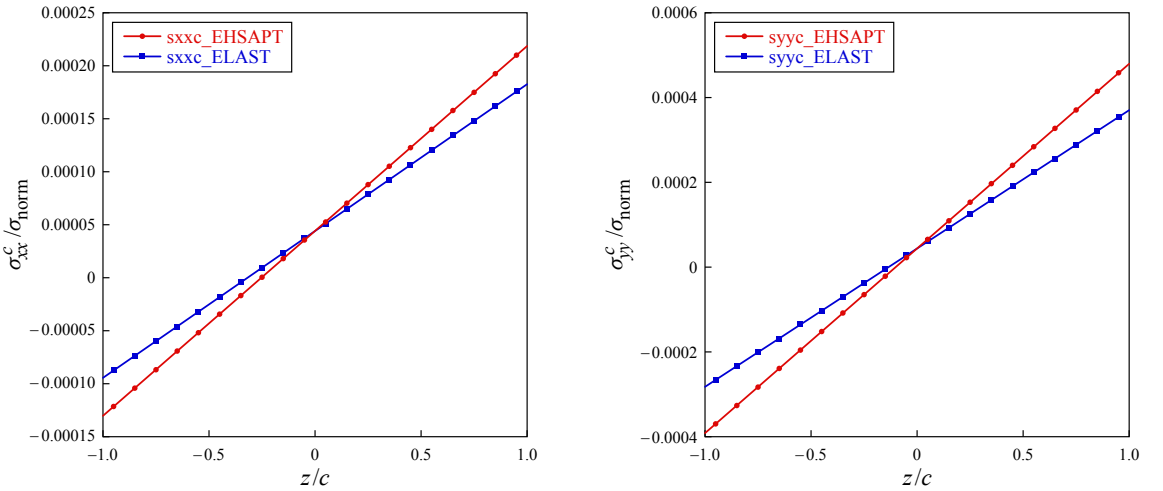**Figure 5.** Transverse displacement w^t at the top face $z = c + f^t$ at $y = \frac{1}{2}b$ for $a = b = 20h_{\text{tot}}$.

Figure 6. Through-thickness distribution in the core of the axial stress: σ_{xx} (left) and σ_{yy} (right) at $x = \frac{1}{2}a$ and $y = \frac{1}{2}b$; case of $a = b = 20h_{\text{tot}}$.

3. Application of EHSAPT to a simply supported sandwich plate: dynamic case

The dynamic case of a simply supported rectangular plate on all four edges is considered and boundary conditions mentioned in (2-1) are applied at $x = 0, a$. Similar boundary conditions can be written for the other two ends of the plate at $y = 0, b$.

The displacements for the dynamic case can be written in the form

$$u_0^t = U^T \cos \frac{m\pi x}{a} \sin \frac{n\pi y}{b} e^{i\omega t}, \quad u_0^c = U^C \cos \frac{m\pi x}{a} \sin \frac{n\pi y}{b} e^{i\omega t}, \quad u_0^b = U^B \cos \frac{m\pi x}{a} \sin \frac{n\pi y}{b} e^{i\omega t}, \quad (3\text{-}1a)$$

$$v_0^t = V^T \sin \frac{m\pi x}{a} \cos \frac{n\pi y}{b} e^{i\omega t}, \quad v_0^c = V^C \sin \frac{m\pi x}{a} \cos \frac{n\pi y}{b} e^{i\omega t}, \quad v_0^b = V^B \sin \frac{m\pi x}{a} \cos \frac{n\pi y}{b} e^{i\omega t}, \quad (3\text{-}1b)$$

$$w^t = W^T \sin\frac{m\pi x}{a} \sin\frac{n\pi y}{b} e^{i\omega t}, \quad w_0^c = W^C \sin\frac{m\pi x}{a} \sin\frac{n\pi y}{b} e^{i\omega t}, \quad w^b = W^B \sin\frac{m\pi x}{a} \sin\frac{n\pi y}{b} e^{i\omega t}, \quad \text{(3-1c)}$$

$$\phi = \Phi \sin\frac{m\pi x}{a} \cos\frac{n\pi y}{b} e^{i\omega t}, \qquad \psi = \Psi \cos\frac{m\pi x}{a} \sin\frac{n\pi y}{b} e^{i\omega t}. \qquad \text{(3-1d)}$$

Substituting equations (3-1) into the governing differential equations [SK 2019] results in a system of eleven equations which are collected to obtain

$$([K] - \lambda[M])\{u_0^b\ u_0^c\ u_0^t\ v_0^b\ v_0^c\ v_0^t\ w^b\ w_0^c\ w^t\ \phi\ \psi\}^T = 0, \text{ where } \lambda = \omega^2, \qquad \text{(3-2)}$$

where $[K]$ and $[M]$ are the stiffness and mass matrices respectively.

3A. *Numerical results and case study.* In this section, the numerical results for several different geometric configurations are presented and a parametric study to analyze the free response of laminated composite plates is carried out. In order to make the comparison with an existing elasticity solution provided by Noor [1973], a simply supported square laminated plate with the face sheets and core constructed from the same material is considered. It should be noted that uniform material properties have been chosen to validate the current formulation against the elasticity solution, which does not exist for sandwich configurations. Two different symmetric layouts with respect to the middle plane such that the fiber orientations of the laminas alternate between $0°$ and $90°$ with respect to the x-axis are studied and compared to the elasticity solution. The following material properties are used:

$$E_1/E_2 = 3, \quad E_2 = E_3, \quad G_{12} = G_{13} = 0.6E_2, \quad G_{23} = 0.5E_2, \quad \nu_{12} = \nu_{13} = \nu_{23} = 0.25.$$

Following the Navier's solution procedure [Reddy 2006] the assumed displacement functions are substituted (3-1) into the governing differential equations [SK 2019], and the resulting eigensystem is solved. The nondimensionalized frequency are evaluated as:
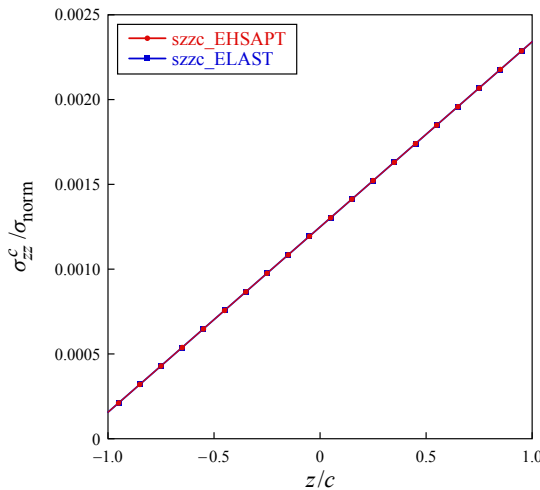
$$\bar{\lambda} = (\omega b^2/h)\sqrt{\rho/E_2},$$

Figure 7. Through-thickness distribution in the core of the transverse normal stress σ_{zz} at $x = \frac{1}{2}a$ and $y = \frac{1}{2}b$; case of $a = b = 20h_{\text{tot}}$.

lamination and # of layers	elasticity	EHSAPT
0/90/0	6.6185	6.56874
0/90/0/90/0	6.6468	6.6521

Table 1. Nondimensionalized fundamental frequencies, $\bar{\lambda} = (\omega b^2/h)\sqrt{\rho/E_2}$ for a simply supported square plate with $a/h = 5$.

where ω is the circular frequency.

Table 1 shows that the results from EHSAPT closely match the elasticity solutions and provide us the necessary basis to verify our results and carry out a parametric study and analyze the variation of the fundamental natural frequency vis-à-vis changes in various geometric and material parameters.

4. Parametric study

The variation of fundamental frequency with respect to the following parameters is studied:

a/h side-to-thickness ratio

t_c/t_f thickness of the core to thickness of face-sheets

a/b aspect ratio

E_1^c/E_2^c degree of orthotropy of the core

E_1^f/E_2^f degree of orthotropy of the flanges

4A. *5-Ply symmetric laminate with typical material properties.* Considering the material properties of individual layers in the flanges and the core are typical of high fibrous composites,

$$E_2^f = E_3^f, \quad G_{12}^f = G_{13}^f = 0.6E_2^f, \quad G_{23}^f = 0.5E_2^f, \quad v_{12}^f = v_{13}^f = v_{23}^f = 0.25,$$
$$E_2^c = E_3^c, \quad G_{12}^c = G_{13}^c = 0.6E_2^c, \quad G_{23}^c = 0.5E_2^c, \quad v_{12}^c = v_{13}^c = v_{23}^c = 0.25.$$

Additionally we consider three different symmetric layouts of the composite sandwich laminate:

- 0/90/core/90/0
- 0/60/core/60/0
- 0/45/core/45/0

Initially, considering the variation of the normalized fundamental natural frequency with the side to thickness ratio for a simply supported square plate with $t_c/t_f = 10$, $E_1^f/E_2^f = 3$ and $E_1^c/E_2^c = 10$, in Figure 8, left, it can be seen that as the side to thickness ratio increases, the natural frequency also starts to increase for all three laminates considered. It can be seen that the highest fundamental natural frequency is achieved in the case of the 0/45/core/45/0 symmetric layout for any given a/h ratio. Moreover, the increase in natural frequency with an increase in side-to-thickness ratio can be explained by the fact that the sandwich plates are not assumed to be infinitely stiff through the thickness since the shear terms are included in the analytical plate model. The effect of the shear deformation results in a decrease in normalized natural frequency. This effect is more pronounced when the thickness, h of the plate increases, which can also be symbolized by an increase in a/h ratio.
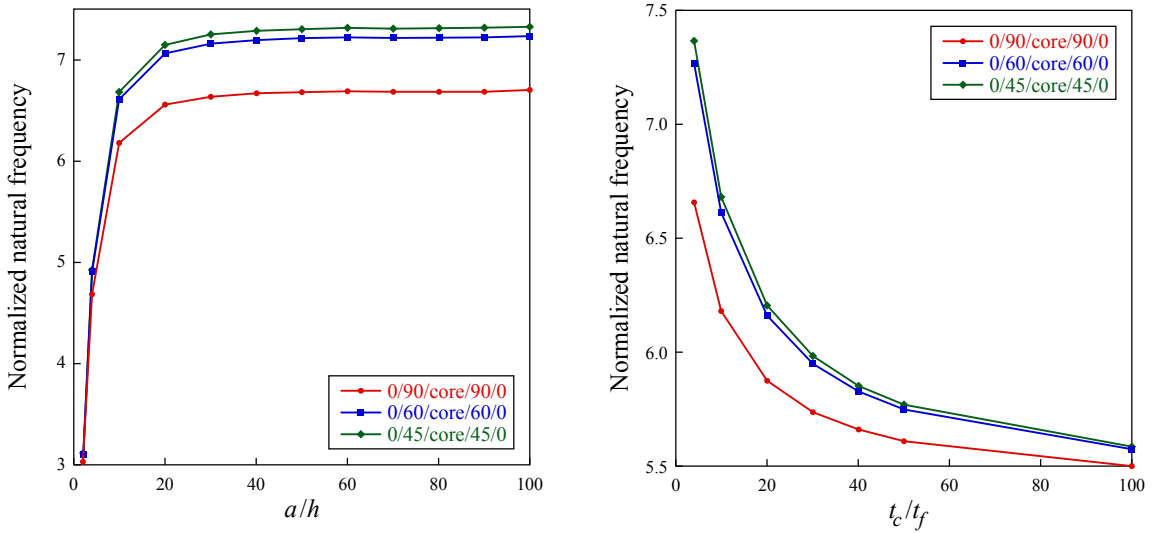
Figure 8. Fundamental natural frequency versus a/h ratio (left) and t_c/t_f ratio (right).

Next, the variation of the normalized fundamental natural frequency with the thickness of the core to thickness of the face-sheets for a simply supported square plate with $a/h = 10$, $E_1^f/E_2^f = 3$ and $E_1^c/E_2^c = 10$ is analyzed and depicted in Figure 8, right. It is known that an increase in stiffness of the sandwich plate results in an increased normalized natural frequency. A similar behavior for various laminates is observed. It can be seen that as the core thickness increases in relation to the thickness of the face-sheets the fundamental natural frequency starts to decrease. Again it can be seen that the highest fundamental natural frequency is achieved in the case of the 0/45/core/45/0 symmetric layout for any given t_c/t_f ratio.

In the next case, the variation of the fundamental natural frequency with the aspect ratio of the simply supported plate with $t_c/t_f = 10$, $a/h = 10$, $E_1^f/E_2^f = 3$ and $E_1^c/E_2^c = 10$ is considered and presented in Figure 9, left. It can be seen that as the aspect ratio increases (that is, as the plate becomes narrower), its fundamental natural frequency starts to decrease. In this case the layout of the laminate does not seem to have a significant effect on the natural frequency of the laminate composite plate.

The effect of variation of the degree of orthotropy of the core for a simply supported square laminated plate with $t_c/t_f = 10$, $a/h = 10$ and $E_1^f/E_2^f = 3$ is shown in Figure 9, right. It can be seen that as the degree of orthotropy of the core increases the fundamental natural frequency of the plate starts to decrease and the isotropic core provides the highest natural frequency for any laminate layout. Again the 0/45/core/45/0 layout seems to provide the highest fundamental natural frequency for any given E_1^c/E_2^c ratio.

Finally, the effect of varying the degree of orthotropy of the flanges for a simply supported square plate with an isotropic core and $t_c/t_f = 10$ and $a/h = 10$ is considered and presented Figure 10. It can be seen that as the ratio E_1^f/E_2^f increases the fundamental natural frequency of the plate also increases and hence it can be concluded that a combination of a isotropic core and highly orthotropic flanges provides the highest fundamental natural frequency.
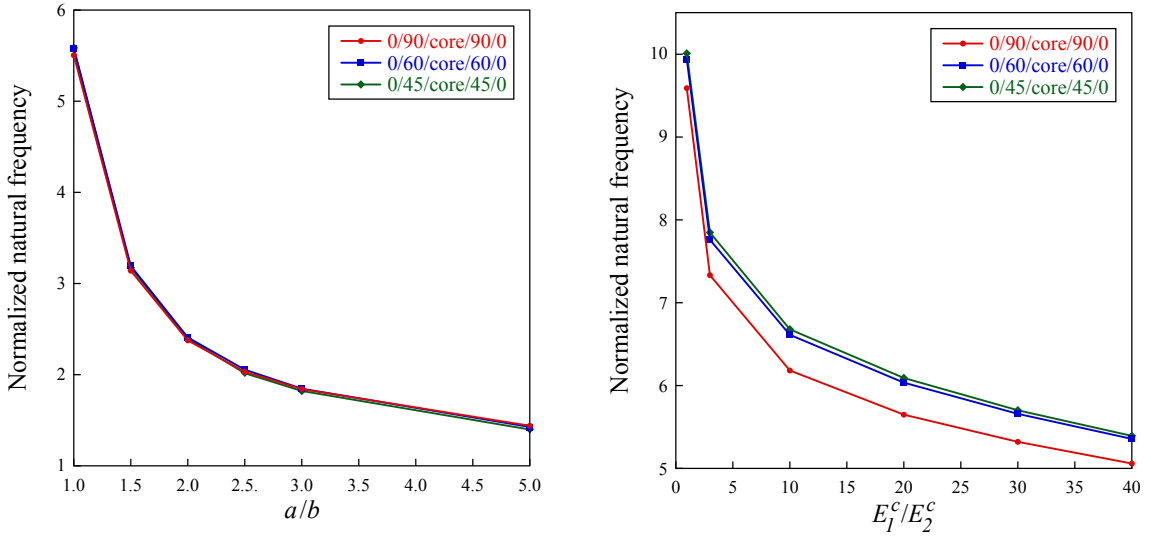
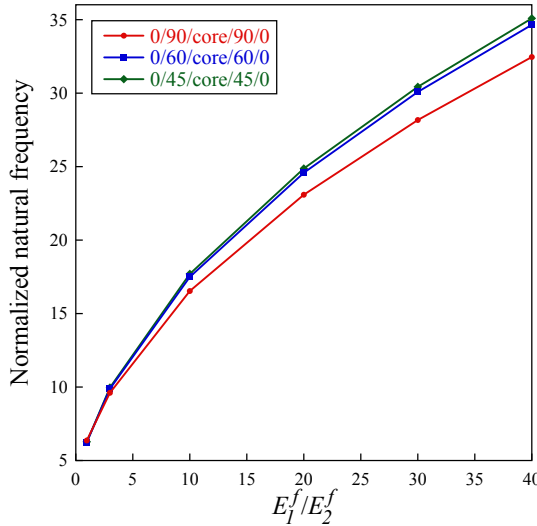**Figure 9.** Fundamental natural frequency versus aspect ratio (left) and E_1^c/E_2^c ratio (right).

Figure 10. Fundamental natural frequency versus variation in the E_1^f/E_2^f ratio.

4B. *3-ply symmetric graphite-epoxy T300/934 laminate.* We now consider a 3-ply laminate graphite-epoxy T300/934 with the following material properties:

- Face sheets:

$$E_1^f = 19 \cdot 10^6 \text{ psi (131 GPa)}, \qquad E_2^f = 1.5 \cdot 10^6 \text{ psi (10.34 GPa)}, \qquad E_2^f = E_3^f,$$

$$G_{12}^f = 1 \cdot 10^6 \text{ psi (6.895 GPa)}, \quad G_{13}^f = 0.90 \cdot 10^6 \text{ psi (6.205 GPa)}, \qquad G_{23}^f = 1 \cdot 10^6 \text{ psi (6.895 GPa)},$$

$$\nu_{12}^f = 0.25, \qquad\qquad\qquad \nu_{13}^f = 0.22, \qquad\qquad\qquad \nu_{23}^f = 0.49,$$

$$\rho^f = 0.057 \text{ lb/inch}^3 \text{ (1627 kg/m}^3\text{)}.$$
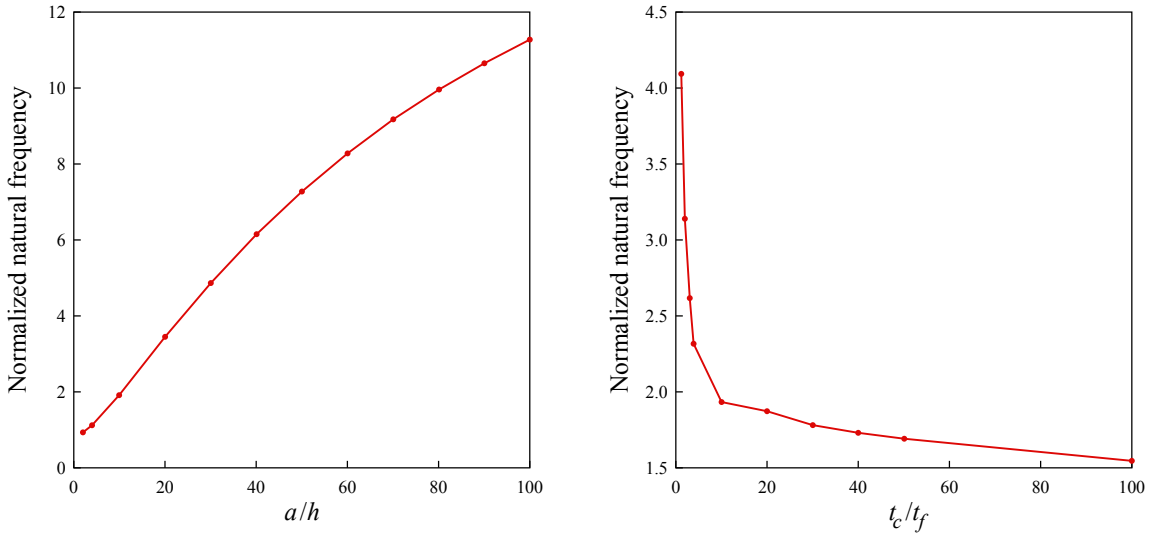
Figure 11. Normalized fundamental frequency versus side-to-thickness ratio a/h (left) and thickness of core to thickness of face sheet t_c/t_f (right) of a simply supported 3-ply square plate.

- Core properties (isotropic):

$$E_1^c = E_2^c = E_3^c = 2G^c = 1000 \, \text{psi} \ (6.89\text{x}10^{-3} \, \text{GPa}),$$

$$G_{12}^c = G_{13}^c = G_{23}^c = 500 \, \text{psi} \ (3.45\text{x}10^{-3} \, \text{GPa}),$$

$$\nu_{12}^c = \nu_{13}^c = \nu_{23}^c = 0,$$

$$\rho^c = 0.3403\text{x}10^{-2} \, \text{lb/inch}^3 \ (97 \, \text{kg/m}^3).$$

Initially, considering the variation of the normalized fundamental natural frequency with the side to thickness ratio (a/h) for a simply supported square plate with $t_c/t_f = 10$. In Figure 11, left, it can be observed that the natural frequency increases as a/h increases. This is because the sandwich plate is considered to be infinitely rigid through the thickness.

Now, considering the variation of the normalized fundamental natural frequency with the thickness of the core to thickness of the face-sheets for a simply supported square plate with $a/h = 10$. In Figure 11, right, it can again be seen that as the core thickness increases in relation to the thickness of the face sheets the fundamental natural frequency starts to decrease.

Finally, considering the variation of the fundamental natural frequency with the aspect ratio of the simply supported plate with $t_c/t_f = 10$ and $a/h = 10$. In Figure 12 as expected, it can be seen that as the aspect ratio increases the fundamental natural frequency starts to decrease. This result again matches the behavior as predicted in Figure 9.

5. Conclusion

This paper presents the applications and validation of extended higher-order sandwich panel theory for plates with arbitrary aspect ratios presented in [SK 2019]. The results have been presented for a
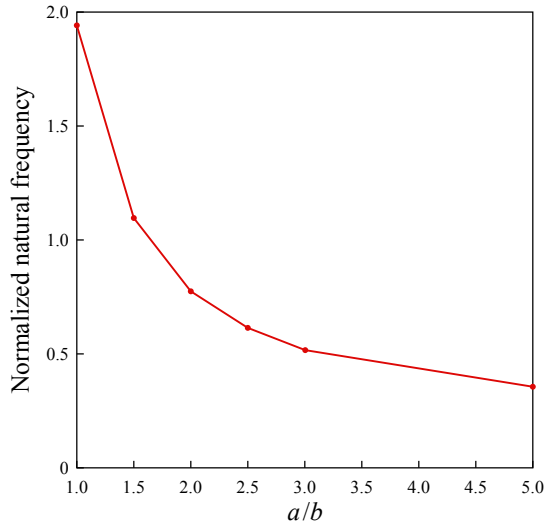
Figure 12. Normalized fundamental frequency versus aspect ratio (a/b) of a simply supported 3-ply plate.

transversely loaded simply supported sandwich panel and are then compared to the classical model, the first-order shear model [Plantema 1966; Allen 1969] and elasticity solutions [Kardomateas and Phan 2011; Kardomateas 2008]. It is quite evident that the EHSAPT theory generates very good results which are in excellent agreement with the elasticity solution. These results also highlight the shortcomings of the incumbent classical and first-order shear models.

It is highlighted that some of the other recently presented higher order sandwich panel theories present very good results for the displacement profile but stresses through the core show inconsistencies when compared to elasticity solutions. The same can be seen by comparing the results obtained by Li and Kardomateas [2008]. It can be seen that his theory generates a very closely matched displacement profile but the transverse normal stress through the core (σ_{zz}^c) does not match the elasticity solution and underestimates the stress at the face sheet and core interface. It is highlighted that through the thickness, transverse normal stress in the core can play a very crucial role in failure modes of the sandwich plate and debonding at the interfaces, local wrinkling and core crushing are some serious repercussions of inaccurate results. The present EHSAPT theory on the other hand not only generates excellent results for the displacement solution but also shows superior agreement with the exact solution for stresses. Therefore, this new theory is expected to have wide implications in the analysis of sandwich plate structures.

Analytical formulations and solutions to the natural frequency analysis of simply supported composite sandwich laminated plates based on a higher-order theory is presented. The displacement field takes into account the compressibility effects in the core which allows us to take the axial, shear and transverse normal stresses in the core into consideration. For laminated composite plates the solutions of this higher-order refined theory are found to be in excellent agreement with the three-dimensional elasticity solution.

A parametric study was then carried out to analyze the effect of varying the various geometric parameters and material properties on the fundamental natural frequency of laminated composite sandwich

plates with three different symmetric layouts. This study could suggest some guidelines for sandwich plate optimal design.

References

[Allen 1969] H. J. Allen, *Analysis and design of structural sandwich panels*, Pergamon, Oxford, 1969.

[Frostig et al. 1992] Y. Frostig, M. Baruch, O. Vilnay, and I. Sheinman, "High-order theory for sandwich-beam behavior with transversely flexible core", *J. Eng. Mech.* (*ASCE*) **118**:5 (1992), 1026–1043.

[Hohe et al. 2006] J. Hohe, L. Librescu, and S. Y. Oh, "Dynamic buckling of flat and curved sandwich panels with transversely compressible core", *Compos. Struct.* **74**:1 (2006), 10–24.

[Kardomateas 2008] G. A. Kardomateas, "Three-dimensional elasticity solution for sandwich plates with orthotropic phases: the positive discriminant case", *J. Appl. Mech.* (*ASME*) **76**:1 (2008), art. id. 014505.

[Kardomateas and Phan 2011]G. A. Kardomateas and C. N. Phan, "Three-dimensional elasticity solution for sandwich beams/wide plates with orthotropic phases: the negative discriminant case", *J. Sandw. Struct. Mater.* **13**:6 (2011), 641–661.

[Li and Kardomateas 2008] R. Li and G. A. Kardomateas, "Nonlinear high-order core theory for sandwich plates with orthotropic phases", *AIAA J.* **46**:11 (2008), 2926–2934.

[Noor 1973] A. K. Noor, "Free vibrations of multilayered composite plates", *AIAA J.* **11**:7 (1973), 1038–1039.

[Phan et al. 2012] C. N. Phan, Y. Frostig, and G. A. Kardomateas, "Analysis of sandwich beams with a compliant core and with in-plane rigidity: extended high-order sandwich panel theory versus elasticity", *J. Appl. Mech.* (*ASME*) **79**:4 (2012), art. id. 041001.

[Plantema 1966] F. J. Plantema, *Sandwich construction: the bending and buckling of sandwich beams, plates, and shells*, Wiley, New York, 1966.

[Reddy 2006] J. N. Reddy, *Theory and analysis of elastic plates and shells*, 2nd ed., CRC, Boca Raton, FL, 2006.

[SK 2019] F. Siddiqui and G. A. Kardomateas, "Extended higher order sandwich panel theory for plates with arbitrary aspect ratios", *J. Mech. Mater. Struct.* **14**:4 (2019).

FAISAL SIDDIQUI: faisals@gatech.edu
Georgia Institute of Technology, Atlanta, GA, United States

GEORGE A. KARDOMATEAS: george.kardomateas@aerospace.gatech.edu
Georgia Institute of Technology, Atlanta, GA, United States

JOURNAL OF MECHANICS OF MATERIALS AND STRUCTURES

msp.org/jomms

Founded by Charles R. Steele and Marie-Louise Steele

Cover photo: Mando Gomez, www.mandolux.com

See msp.org/jomms for submission guidelines.

PUBLISHED BY

mathematical sciences publishers

nonprofit scientific publishing

http://msp.org/